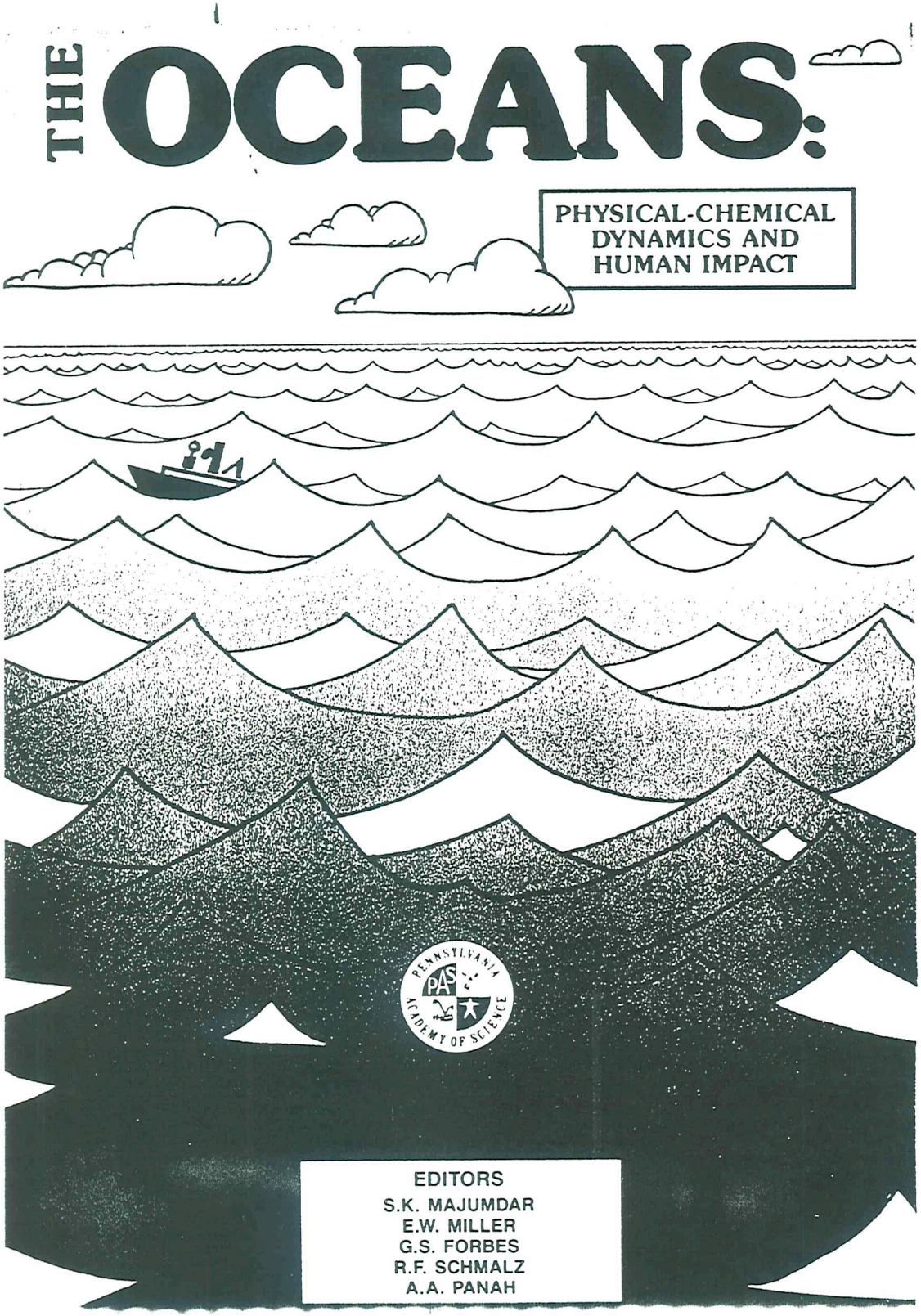

The Oceans: Physical-Chemical Dynamics and Human Impact. Edited by S.K. Majumdar, E.W. Miller, G.S. Forbes, R.F. Schmalz and Assad A. Panah.

Chapter Two

SIMULATING THE OCEANIC CIRCULATION WITH ISOPYCNIC-COORDINATE MODELS

RAINER BLECK and ERIC P. CHASSIGNET

Division of Meterology and Physical Oceanography
University of Miami
Miami, FL 33149

INTRODUCTION

Numerical modeling of geophysical fluid systems using electronic computers began approximately four decades ago. Until the mid- to late 1960s, ocean model development lagged significantly behind that of atmospheric models. A number of reasons (apart from societal needs) can be cited for this lag, among them the inherently greater complexity of circulation systems confined to closed basins, a highly nonlinear equation of state for seawater, and the lack of three-dimensional synoptic observations for ocean model initialization and verification. Furthermore, the computing power required to resolve the relevant hydrodynamic instability processes is far greater in the ocean than in the atmosphere because such processes occur on much smaller scales in the ocean. The above factors, taken together, imply that a major commitment of institutional resources was required in the past to mount a credible oceanic modeling effort. Thus, oceanic modeling never became a "cottage industry" like numerical weather prediction. Fiscal constraints often prohibited the luxury of a "duplication of efforts," and thus steered the oceanographic community away from model diversity. Only now, with supercomputers being within easy reach of university researchers, can such a diversity be achieved and should, in fact, be encouraged.

Before a system of differential equations can be solved on a computer, it must be converted into an algebraic system, a process which entails numerous

approximations. Models have become "better" over the years not only because our knowledge of physics has improved, but also because modern computers permit a more faithful representation of the differential equations by their algebraic analogs. Specifically, the discretization or "truncation" error introduced when approximating differentials by finite differences decreases as advances in computing speed and memory size allow smaller and smaller mesh sizes.

Rather than counting on future computers that ultimately will allow algebraic and differential equations to converge, numerical modelers try to reduce the truncation error in their model on existing machines by using sophisticated ("higher-order") approximations or distributing a fixed number of grid points in physical space such that they optimally define the spatial structure of the modeled system. For example, representation of flow in the x, y plane near a ragged coastline can be improved by placing grid points at the intersections of curvilinear coordinate lines hugging the coast. Map projections such as the Mercator projection can be used as a tool to reduce the mesh size toward higher latitudes to account for the general poleward decrease in eddy size.

Another method of reducing the truncation error in geophysical fluid modeling entails replacing the independent variable z in the governing equations[1] by another variable. For example, numerical weather prediction models often use the ratio of *in-situ* and surface pressure ("σ") as vertical coordinate to improve the smoothness of the numerical solution near topographic obstacles.[2] Ocean models based on σ coordinates are gaining popularity,[3,4] ironically at a time when the atmospheric modeling community is beginning to seek alternatives to the σ system because of problems with computing the horizontal pressure force on coordinate surfaces following the bottom relief.

Mixing in stratified fluids where buoyancy effects play a role takes place predominantly along isopycnic or constant-density surfaces (*potential* density surfaces, to be precise).[5] If the conservation equations for salt and temperature are discretized in x, y, z space, that is, if the three-dimentional vectorial transport of these quantities is numerically evaluated as the sum of scalar transports in x, y, z direction, experience shows that it is virtually impossible to avoid diffusing the transported variables in those same directions. Thus, regardless of how the actual mixing term in the conservation equations is formulated, numerically induced mixing is likely to have a cross-isopycnal ("diapycnal") component which may well overshadow the diapycnal processes occurring in nature. This is known to have serious consequences for long-term climate simulations.

Isopycnic-coordinate modeling seeks to eliminate this type of truncation error by transforming the dynamic equations from x, y, z to x, y, ρ coordinates and discretizing them on an x, y, ρ model grid. Transport in x, y direction then takes place in the model on isopycnic surfaces, and the associated numerical diffusion has no diapycnal component. Transport in z direction translates into transport along the ρ axis and can be entirely suppressed if so desired; that is, it also has no unwanted diapycnal component. As a result, spurious heat exchange between warm surface waters and cold abyssal waters does not occur in isopycnic models, nor does horizontal heat exchange across sloping isopycnals such as those marking the Gulf Stream front.

A second advantage of isopycnic coordinates is their tendency to concentrate grid points vertically in regions where grid resolution is needed most. The near-geostrophic balance characterizing large-scale oceanic motion implies that horizontal jet-like currents must be supported by inclined and tightly packed density surfaces. By their very nature, grid points attached to isopycnals congregate in such so-called frontal zones and provide optimal resolution for the current and the density contrast supporting it.

There is a price to be paid for the advantages outlined above. The ocean, when viewed in x, y, ρ space, has a ragged, sloping upper boundary because isopycnals intersect the sea surface. Thus, coordinate layers sandwiched between near-surface isopycnals and the sea surface form wedges in physical space whose sharp edge marks the outcrop line of the respective isopycnal. This also happens where a subsurface coordinate layer intersects a topographic obstacle. The requirement to inflate and deflate these wedges in an orderly fashion while solving the mass conservation equation (also called the layer thickness tendency equation) is a complicated and not yet completely solved numerical problem. Other shortcomings of the isopycnic coordinate system worth mentioning are the lack of vertical grid resolution in neutrally stable water columns and the nonexistence of a reference pressure-independent definition of the potential density of seawater.

It is fair to say that there is no "best" choice of vertical coordinate in a geophysical fluid model because the solutions of the discretized finite-difference equations should all converge toward the solutions of the differential equations as mesh size goes to zero. Each coordinate system is afflicted with its own set of truncation errors whose implications sometimes become known only after extended experimentation.

ISOPYCNIC SURFACES AND MODELING

Perhaps the most elegant way to construct a 3-dimensional density-coordinate numerical model is to form a stack of 2-dimensional shallow-water models, arranged so that lighter isopycnic layers rest on top of denser layers. The resulting discrete-layer structure is a valid finite-difference approximation to the continuous equations transformed to density coordinates. The fact that a density-coordinate *layer* model has an exact physical analog (at least as far as vertical discretization is concerned) makes this a very attractive concept in model-building. Each layer is characterized by a constant value of density and is governed by dynamic equations resembling the shallow-water equations. The layers interact even in the inviscid limit through hydrostatically transmitted pressure forces.

As mentioned earlier, the advantages of isopycnic-coordinate representation are offset by numerical difficulties encountered where interior density surfaces come into contact with either the ocean surface or the ocean bottom, both of which are treated for practical reasons as additional coordinate surfaces. A hybrid, quasi-isopycnic model can avoid such coordinate intersections by locally reverting to a Cartesian coordinate representation wherever minimum isopycnic grid-point separation in the vertical cannot be maintained.[6] By contrast, a pure isopycnic model

depicts outcrop lines as boundaries between regions of zero and nonzero isopycnic layer thickness and solves the mass continuity equation in such a way that the collapse of a layer to zero thickness does not cause numerical instability.[7] Two algorithms, the Flux Corrected Transport (FCT) scheme[8] and the MPDATA scheme,[9] have been found to be well suited for this purpose![10]

Diabatic forcing of models whose coordinate layers maintain their density requires translating density tendencies $d\rho/dt$ into vertical mass fluxes across layer interfaces. In order to accommodate numerically a variety of physical processes occurring in the ocean's surface mixed layer, the uppermost coordinate layer in an isopycnic-coordinate oceanic general circulation model (OGCM) is usually defined as a *non*-isopycnic layer in which termodynamic variables are allowed to vary continuously in x, y, and t. The depth of the mixed layer is typically determined by assuming that sources and sinks of turbulence kinetic energy, such as wind stirring, buoyancy changes at the surface, and entrainment of denser water from below, balance at all times. Since ocean-atmosphere heat transfer has a large effect on the rate and sign of buoyancy production, the mixed-layer depth varies markedly in the course of a year. Consequently, the mixed layer must be allowed to exchange mass with underlying isopycnic layers. This process is referred to as mixed layer entrainment/detrainment.

The response of the ocean to changes in atmospheric conditions, both man-made and natural, is one of the central topics of climate research today. Processes that determine the thermal structure of the thermocline, its motion field, and its buffering capacity are among the topics being studied. Many of these investigations have been inspired by the ventilated thermocline theory![11] Analytic solutions can be derived for the flow in isopycnic layers forced by density and potential vorticity boundary conditions at the bottom of the Ekman layer in regions of downward Ekman pumping (subduction). Isopycnic modeling opens the door for a generalization of these results, because it allows a coupling of the subduction mechanism with the important process of mixed-layer entrainment and detrainment.

The specific numerical problem posed in the isopycnic framework by mixed-layer entrainment/detrainment is that only a finite number of constant-density layers are available to accept the detrained water (which, as long as it resides in the mixed layer, is allowed to have a density varying continuously in space and time). Some errors in the timing and the rate of detrainment, and consequently in the potential vorticity of the detrained water masses, are therefore inevitable if the model is run in very low vertical resolution mode. How significant these errors are compared to the truncation errors encountered in traditional z-coordinate models using the same number of grid points in the vertical is difficult to assess. There is reason to believe, though, that a Cartesian model with a comparable number of grid points in the vertical would be unable to simulate the annual cycle of mass exchange between the thermocline and the mixed layer with the same degree of realism.

A MODEL OVERVIEW

In this section, we describe the salient features of an isopycnic-coordinate model

developed at the University of Miami. Similar efforts have been undertaken at the Florida State University;[12,13] the Naval Research Laboratory;[14,15] Nova University;[16] Oregon State University[17] and the Hamburg Max-Planck Institute;[18] to name a few. While we have attempted to make the description as self-contained as possible, the reader is referred for technical details to previous publications.[19,20,21]

Contrary to some wind-driven isopycnic models which gain computational efficiency by keeping the lowermost coordinate layer at rest, thereby eliminating barotropic gravity waves, the present model permits motion in all layers and time-integrates the barotropic flow component in "split-explicit" mode. With motion being allowed in the abyssal layers, much of the development effort has been directed at stabilizing the numerical solution in places where the flow interacts with topography. Another challenge was the development of transport algorithms that maintain their conservative properties, including positive-definiteness, in the presence of significant spatial and temporal variations in layer thickness.

Governing Equations

The Miami model is a primitive-equation model containing 4 prognostic equations - one for the horizontal velocity vector, a mass continuity or layer thickness tendency equation, and two conservation equations for salt and heat. The equations, written here for a generalized vertical coordinate "s" to make them formally applicable to both the isopycnic domain and the surface mixed layer,[22] are

$$\frac{\partial \mathbf{v}}{\partial t_s} + \nabla_s \frac{\mathbf{v}^2}{2} + (\zeta + f)\mathbf{k} \times \mathbf{v} + \left(\dot{s}\frac{\partial p}{\partial s}\right)\frac{\partial \mathbf{v}}{\partial p} + \nabla_\alpha M = -g\frac{\partial \tau}{\partial p} + \left(\frac{\partial p}{\partial s}\right)^{-1} \nabla_s \cdot \left(\nu \frac{\partial p}{\partial s} \nabla_s \mathbf{v}\right) \quad (1)$$

$$\frac{\partial}{\partial t_s}\left(\frac{\partial p}{\partial s}\right) + \nabla_s \cdot \left(\mathbf{v}\frac{\partial p}{\partial s}\right) + \frac{\partial}{\partial s}\left(\dot{s}\frac{\partial p}{\partial s}\right) = 0 \quad (2)$$

$$\frac{\partial}{\partial t_s}\left(\frac{\partial p}{\partial s}T\right) + \nabla_s \cdot \left(\mathbf{v}\frac{\partial p}{\partial s}T\right) + \frac{\partial}{\partial s}\left(\dot{s}\frac{\partial p}{\partial s}T\right) = \nabla_s \cdot \left(\nu \frac{\partial p}{\partial s}\nabla_s T\right) + \mathcal{H}_T \quad (3)$$

Here, $\mathbf{v} = (u, v)$ is the horizontal velocity vector, p is pressure, T represents any one of the model's thermodynamic variables (temperature, salinity, buoyancy), $\alpha = \rho^{-1}$ is the specific volume, $\zeta = \partial v/\partial x - \partial u/\partial y$, is the relative vorticity, $M \equiv gz + p\alpha$ is the Montgomery potential, gz is the geopotential, f is the Coriolis parameter, $\mathbf{k}$ is the vertical unit vector, ν is a variable eddy viscosity coefficient, and τ is the wind- and/or bottom drag induced shear stress vector. H_T represents the sum of the diabatic source terms acting on T. Subscripts indicate which variable is held constant during partial differentiation. Distances in x, y direction, as well as their time derivatives $\dot{x} \equiv u$ and $\dot{y} \equiv v$, are measured in the projection onto a horizontal plane, a convention which eliminates metric terms related to the slope of the s surface.[22]

Metric terms created when terms involving $(\nabla\cdot)$ or $(\nabla\times)$ are evaluated in a non-Cartesian grid (e.g., in spherical coordinates) can be formally eliminated by evaluating ζ and horizontal flux divergences in (1) – (3) as line integrals around individual grid boxes. Note that applying ∇ to a scalar, such as $v^2/2$ in (1), does not give rise to metric terms.

After vertical integration over a coordinate layer bounded by two surfaces s_{top}, s_{bot} (the ocean surface, the bottom of the mixed layer, the sea floor, and all isopycnic layer interfaces are s surfaces in this context), the continuity equation (2) becomes a prognostic equation for the layer weight per unit area, $\Delta p = p_{bot} - p_{top}$:

$$\frac{\partial}{\partial t_s}\Delta p + \nabla_s\cdot(\mathbf{v}\Delta p) + \left(\dot{s}\frac{\partial p}{\partial s}\right)_{bot} - \left(\dot{s}\frac{\partial p}{\partial s}\right)_{top} = 0. \tag{4}$$

The expression $(\dot{s}\partial p/\partial s)$ represents the vertical mass flux – taken to be positive if in $+p$ or downward direction – across an s surface.

Multiplication of (1) by $\partial p/\partial s$ and integration over the interval (s_{top}, s_{bot}), followed by division by $\Delta p/\Delta s$, changes the shear stress term in that equation into

$$\frac{g}{\Delta p}(\tau_{top} - \tau_{bot})$$

while the lateral momentum mixing term integrates to

$$(\Delta p)^{-1}\nabla_s\cdot(\nu\Delta p\,\nabla_s\mathbf{v}). \tag{5}$$

All other terms in (1) retain their formal appearance.

Wind-induced stress is assumed to be zero at the bottom of the mixed layer, which therefore must not be allowed to become shallower than the Ekman layer. Bottom stress is prorated among coordinate layers in accordance with the assumption that it linearly decreases from $-\rho c_D|\mathbf{v}|\mathbf{v}$ to zero over the lowest $10m$ of the water column. v in this formula is the velocity vector averaged over the lowest $10m$.

The layer-integrated form of (3) is

$$\frac{\partial}{\partial t}T\Delta p + \nabla_s\cdot(\mathbf{v}T\Delta p) + \left(\dot{s}\frac{\partial p}{\partial s}T\right)_{bot} - \left(\dot{s}\frac{\partial p}{\partial s}T\right)_{top} = \nabla_s\cdot(\nu\Delta p\,\nabla_s T) + \gamma_T. \tag{6}$$

The above prognostic equations are complemented by diagnostic equations including the hydrostatic equation

$$\frac{\partial M}{\partial \alpha} = p, \tag{7}$$

an equation of state linking T, S to α, and a turbulence kinetic energy balance equation[19] yielding the depth of the mixed layer.

Horizontal and Vertical Grid

Isotropy in horizontal grid resolution is considered an important aspect of model

numerics; therefore, the equations are solved on a regular mesh superimposed on a conformal (presently: Mercator) projection of the earth's surface. Thus, for a mesh size of n degrees longitude the mesh size in meridional direction at latitude φ is $(n\cos\varphi)$ degrees. The map-scale factor is a function of φ, but not of direction: grid squares on the map project onto (nearly) square areas on the sphere.

Velocity and mass field variables are staggered horizontally such that $u(v)$ grid points are positioned halfway between mass grid points in x (y) direction. This staggering arrangement, known as the Arakawa C grid, is not considered optimal for coarse-mesh (noneddy-resolving) models,[21] but was chosen with eddy-resolving applications in mind.

Thermodynamic variables and the velocity vector v are treated as "layer" variables which are vertically constant within layers but change discontinuously across layer interfaces. p, z and $\dot{s}\partial p/\partial s$, on the other hand, are "level" variables defined on interfaces. Since M only changes according to (7) where α changes vertically, M is a layer variable.

Time Differencing Scheme

The time step permissible when solving hyperbolic differential equations such as those governing fluid motion is limited by the requirement that no signal may travel faster than one grid interval per time step. By far the fastest signals in the ocean are those associated with barotropic gravity waves; these travel nearly 20 times faster than any other signal. Since barotropic motion in a weakly stratified medium is nearly independent of depth, barotropic wave propagation is essentially a 2-dimensional process. As mentioned earlier, the Miami model uses a split-explicit scheme[20] to circumvent the limitation posed by barotropic gravity waves on the permissible time step for advancing the 3-dimensional model fields. The barotropic flow field in the model is separated from the rest of the solution and advanced in time in a separate 2-dimensional "sub"-model using a very small time step.

Explicit integration of the barotropic mode was not only found to be faster than the traditional "rigid-lid" scheme, which eliminates barotropic gravity waves altogether but requires the solution of a Poisson equation for the barotropic stream function at each time step, but also has the advantage of producing a sea-surface height field allowing direct comparison with radar altimetry data.

Liberal use is being made in the model of the time-splitting concept. For example (6), is actually decomposed into 4 separate equations which in turn advect the T field horizontally and vertically, diffuse it, and force it diabatically. Vertical advection, being caused in part by cabbeling (defined below) and by mixed-layer entrainment/detrainment, is itself a 2-step process.

Isopycnal Outcropping

Outcropping of isopycnic coordinate layers is the Achilles' heel of isopycnic modeling. The modeling philosophy employed in the Miami model is to allow each isopycnic layer to exist at every (x, y) point in the model domain, but also to allow

it to become massless or dynamically "invisible".' Inflation or deflation of each layer, and thus the geographic location where the layer outcrops at a given time, is entirely controlled by the interplay between the continuity and momentum equations. Special algorithms referred to earlier[10] are required to make this scheme work; these are somewhat more expensive than conventional finite-difference methods for solving the mass continuity equation but do not require a special bookkeeping effort[18] to keep track of layer outcrop lines or time-dependent lateral boundaries in individual layers. Note that the presence in the model of a nonisopycnic surface layer does not alleviate the outcropping problem: isopycnic layers in the present model outcrop into the mixed layer.

Variable bottom topography requires that the layers also be allowed to intersect the ocean bottom. The bottom intersection problem is numerically similar to the surface outcrop problem.

Surface Forcing Functions

The model ocean can be driven by a variety of forces emulating those found in nature. These forces are (*i*) large-scale wind stress; (*ii*) small-scale mechanical stirring; (*iii*) two imposed (*i.e.*, model-state independent) fluxes representing solar radiation and precipitation; and (*iv*) two relaxation boundary conditions representing sensible heat flux and evaporation. Salinity varies according to the balance between evaporation and imposed rainfall. This type of salinity forcing, which differs from the commonly employed Newtonian relaxation toward observed surface salinity, is prefered for two reasons: (*a*) a salinity relaxation boundary condition is nonphysical because evaporation is virtually independent of surface salinity and precipitation is totally so; (*b*) imposed boundary fluxes are more likely to generate unrealistic salinity features, thus the model's reaction to such features provides valuable insight into its ability to simulate climates different from the present one.

Mixed Layer

The modes of interaction between the thermodynamically active mixed layer and the interior isopycnic coordinate layers are thoroughly documented elsewhere[9,21,24] The main problem is that water to be discharged from the mixed layer into underlying layers during periods of surface heating generally does not match the density of an interior layer. Thus, the model mixed layer is too deep most of the time, *i.e.*, it contains a certain amount of "fossil" mixed-layer water. This water is being heated in the model at the same rate as the "true" mixed layer and thus remains indistinguishable from the latter. For obvious physical reasons, the heat required to warm the fossil mixed layer cannot be taken from the atmosphere; rather, it is taken from the bottom of the fossil mixed-layer column. The heat loss there creates water dense enough to match an interior coordinate layer, allowing it to be detrained into that layer. The unknown in this problem is the relative thickness of the heated and cooled portions of the fossil mixed layer.

The model is able to dispose of the fossil mixed layer each time the mixed-layer density during springtime warming matches the density of an interior coordinate layer. This gives rise to sudden detrainment events which are numerically undesirable. They represent a special truncation error in the sense that they can be suppressed by reducing the mesh size in ρ space, *i.e.*, by adding more layers.

Equation of State

The equation of state for seawater currently used in the Miami model approximates density by a polynomial linear in salinity and of 3rd-degree in temperature.[25] The mixed-layer detrainment algorithm requires that this equation be inverted to yield T as a function of S and ρ. Finding the roots of a 3rd-degree polynomial involves repeated calls to trigonometric functions to avoid complex-valued arithmetic and is therefore rather time-consuming. Of the three roots of the polynomial, the one guaranteed to be real lies near 180°C and is therefore nonphysical. The other two roots, if they exist, form a pair straddling a temperature value in the range -3° to -5°C where ρ for seawater reaches its maximum; the root above this value is the physical one and is used in computing $T(\rho, S)$.

In the present model implementation, no distinction is made between density and potential density, and the effect of pressure on these quantities is ignored. These simplifications can (and, in fact, do) lead to erroneous conclusions about the static stability of abyssal water masses marked by vertical salinity gradients. One possible solution to this problem is to reference potential density to 2000m depth rather than the surface.

The nonlinearity of the equation of state causes the mixture of two water parcels of equal density but different temperature and salinity to be denser than the original parcels. The German verb *kabbeln*, which is used to describe this phenomenon, suggests that such mixing usually produces a "choppy" or fine-grain vertical velocity field. Cabbeling in a coarse-mesh ocean model is therefore a severely aliased process.

In an isopycnic coordinate model, cabbeling generates a positive vertical velocity component $d\rho/dt$, i.e., a gradual transfer of mass from each coordinate layer to the one beneath it. In the Miami model, the cabbeling process is treated as part of the more general problem of maintaining the reference density in coordinate layers where the T, S fields evolve independently of each other.

Thermodynamic Equations

As stated earlier, the model accomodates two independent thermodynamic variables. The prognostic equations for these variables (buoyancy b and salinity S in the mixed layer, temperature T and S in the interior) are all of the form (6). Horizontal advection (note that "horizontal" translates into isopycnal everywhere in the model except in the mixed layer) is handled by the conservative, monotony-preserving, version of the Smolarkiewicz transport scheme.[26] The diabatic source term H_T in (3) symbolizes three different processes - cabbeling, diabatic diffusion, and mixed-layer entrainment/detrainment. Due to the need to keep density

constant in isopycnic layers, all diabatic processes must be converted into vertical mass fluxes $\dot{s}\partial p/\partial s$. Thus, in the absence of diabatic processes, no transport of thermodynamic variables takes place across layer interfaces, either explicitly or implicitly.

Continuity Equation

The split-explicit time integration scheme requires that changes in layer thickness caused by the barotropic velocity component $\bar{v}$ be evaluated separately from those caused by the baroclinic component v'. The barotropic velocity is approximated in the model by the vertically averaged velocity $\bar{v} = (\Sigma_k v_k \Delta p_k) / (\Sigma_k \Delta p_k)$ where k is the coordinate layer index and the summation extends over all layers. The terms "barotropic" and "depth-averaged" will be used here interchangeably. The deviation of the actual velocity in a layer from the depth-averaged velocity will be termed "baroclinic".

Depth-independent motion stretches or shrinks the water column uniformly; that is, it changes the thickness Δp of a layer in proportion to Δp itself. This suggests that the individual effects of $\bar{v}$ and v' on Δp may be isolated by setting $\Delta p = (1 + \eta)\Delta p'$ where temporal changes in $(1 + \eta)$ and $\Delta p'$ are caused, respectively, by mass flux divergences associated with $\bar{v}$ and v'. Hence, η is independent of k while $p_b' \equiv \Sigma_k \Delta p_k'$ is time-independent.

The layer-integrated continuity equation (8), with vertical mass fluxes omitted for brevity, can now be written as

$$\frac{\partial}{\partial t_a}[(1 + \eta)\Delta p_k'] + \nabla_a \cdot [(\bar{v} + v_k')(1 + \eta)\Delta p_k'] = 0 \tag{8}$$

Summation over k and linearization yields the barotropic continuity equation

$$\frac{\partial}{\partial t}(p_b'\eta) + \nabla \cdot [\bar{v}\Delta p_b'] = 0 \tag{9}$$

Subtracting (9) from (8) and approximating $(1 + \eta)$ by 1 yields the baroclinic continuity equation

$$\frac{\partial}{\partial t_a}\Delta p_k' + \nabla_a \cdot (v_k \Delta p_k') = \frac{\Delta p_k'}{p_b'}\nabla \cdot (\bar{v} p_b') \tag{10}$$

where $v_k = \bar{v} + v_k'$. Note that replacing $(1 + \eta)$ by 1 in both (9) and (10) preserves the condition $\partial(\Sigma_k \Delta p_k')/\partial t = 0$.

The corresponding split of the momentum equations into their barotropic and baroclinic parts will be discussed in the following section.

Momentum Equations

Even though the nonlinear terms in (1) play no significant role in coarse-mesh basin-scale simulations, the equations are written in their fully nonlinear form to accomodate fine-mesh applications. The Coriolis and nonlinear terms conserve potential vorticity and potential enstrophy except in the vicinity of zero layer thickness zones.[20] The mixing terms are written in conservative form and use an eddy viscosity that reverts from a constant value to one proportional to the total deformation in regions of large horizontal shear.[27] Specifically, the eddy viscosity used in isopycnal mixing of momentum is defined as

$$\nu = max\left(u_d \Delta x, \eta[(u_x - v_y)^2 + (v_x + u_y)^2]^{1/2}\Delta x^2\right) \tag{11}$$

where Δx is the mesh size, subscripts denote partial derivatives, u_d is a background diffusive velocity, and η is a dimensionless factor.

Near steep bottom topography, the horizontal pressure force $\nabla_p M$ is computed in spatially non-centered form to avoid extrapolating pressure to underground grid points. Details of the scheme, which basically infers a layer-depth weighted average of $\nabla_p M$ from points surrounding the grid point in question, are provided elsewhere.[20]

Lateral sidewalls are usually chosen to coincide with grid points of the *normal* velocity component to allow enforcement of the kinematic boundary condition. In the C grid, this implies that the tangential velocity grid point nearest a sidewall is displaced from the wall by half a grid distance. A "mirror image" of this grid point on the opposite side of the wall is needed to solve the momentum, equation at the inside point. Depending on how one defines the velocity at the mirror image point, one can run a C grid model with free-slip or no-slip lateral boundary conditions.

The convention of extending coordinate layers intersecting the ocean bottom as massless layers all the way to the coast is followed. This convention, in conjunction with a layer depth-weighted lateral mixing formulation, makes it nearly impossible to communicate lateral sidewall drag to, say, grid points in the abyssal ocean next to the continental rise. A "submerged sidewall" boundary condition has been developed to remedy this problem.[20]

A barotropic momentum equation is needed to complement (9) in the 2-dimensional sub-model for the barotropic gravity wave field. Due to the small amplitude of these waves, the equation for $\bar{v}$ is stated in the simple linearized form

$$\frac{\partial \bar{v}}{\partial t} + f\mathbf{k} \times \bar{v} + \alpha_0 \nabla(p_b'\eta) = \frac{\partial \bar{v}^*}{\partial t} \tag{12}$$

The term on the right-hand side is a source term for barotropic momentum. It arises during the solution of the v' equation which one obtains by subtracting (12) from (1):

$$\frac{\partial v_k'}{\partial t_a} + \nabla_a \frac{v_k^2}{2} + (\zeta + f)\mathbf{k} \times v_k - f\mathbf{k} \times \bar{v} + \left(\dot{s}\frac{\partial p}{\partial s}\right)\frac{\partial v_k}{\partial p} + \nabla_a(M - \alpha_0 p_b'\eta) =$$
$$-g\frac{\partial \tau}{\partial p} + \left(\frac{\partial p}{\partial s}\right)^{-1}\nabla_a \cdot \left(\nu\frac{\partial p}{\partial s}\nabla_a v_k\right) - \frac{\partial \bar{v}^*}{\partial t} \tag{13}$$

The term in question is added here to assure that $\Sigma_k v_k' \Delta p_k'$ remains zero at all times. It is evaluated as a residual after (13) has been solved in all model layers.

Subgrid-Scale Mixing

Let Z denote one of the prognostic variables in the model. Since the finite-difference analog of the product $\nu\partial Z/\partial x$ is numerically equivalent to the finite-difference analog of $u_d\partial Z$ (where ∂Z is the Z difference between neighboring grid points, u_d is a "diffusive flux velocity" of magnitude $\nu/\partial x$, and ∂x is the grid size), the practice of specifying u_d rather than ν as the parameter controlling isopycnal mixing was adopted. Setting u_d constant throughout the model domain has the advantage of removing any geographic bias from the relative weight of diffusive and advective processes in shaping the character of the numerical solution. The u_d value also provides a convenient measure of the degree to which diffusion overshadows advection.

Subgrid-scale turbulent flux terms in the prognostic differential equations formally result from Reynolds averaging of the various nonlinear flux terms. Since the term $\nabla\cdot(v\Delta p)$ in (4) is nonlinear, it would seem inconsistent not to add a "thickness diffusion" term to (4). Following the parameterization of subgrid-scale fluxes in the other model equations, the turbulent thickness diffusion term is expressed as $-\nabla\cdot(\nu\nabla\Delta p)$. In order to avoid injecting mass into areas where Δp vanishes due to layer outcropping or intersection with bottom topography, and to prevent thickness smoothing from changing the total weight of a column, thickness smoothing is actually implemented in the model in the form of "interface smoothing". Special precautions are followed to avoid smoothing interfaces coinciding with the sea floor.

Diapycnal Mixing

The diapycnic mixing algorithm in the Miami model is a simplified version of the algorithm developed by Hu.[28] Let θ be the variable that serves as vertical coordinate in the model (potential density), and let $F = K_d\partial\theta/\partial z$ be a parameterization of the vertical turbulent buoyancy flux $\overline{w'\theta'}$. Diapycnal gradients, i.e., gradients normal to θ surfaces, are approximated in the model by gradients in z direction.

To solve the diffusion equation

$$\left(\frac{\partial\theta}{\partial t}\right)_z = \frac{\partial}{\partial z}\left(K_d\frac{\partial\theta}{\partial z}\right) \tag{14}$$

in an (x,y,θ) reference frame, the roles of θ and z as dependent and independent variables must be reversed. This is done through the identity

$$\left(\frac{\partial a}{\partial b}\right)_c\left(\frac{\partial b}{\partial c}\right)_a\left(\frac{\partial c}{\partial a}\right)_b = -1.$$

which changes (14) into

$$\left(\frac{\partial z}{\partial t}\right)_\theta = -\frac{\partial F}{\partial\theta}\,; \qquad F = K_d\frac{\partial\theta}{\partial z}. \tag{15}$$

The above equation is solved in individual grid columns subject to the boundary conditions $F=0$ at top and bottom, expressing conservation of total θ in each column.

Since (15) requires knowledge of vertical F derivatives on layer interfaces, the fluxes F themselves must be *layer* variables. Physical intuition dictates that these fluxes, to first order, should be inversely proportional to isopycnal layer thickness. However, the possible presence of massless and near-massless layers in the water column requires special measures to insure boundedness of the finite-difference estimates of $\partial\theta/\partial z$. We achieve boundedness by formulating $\partial\theta/\partial z$ in terms of θ values representing integrals over a finite depth interval Δz.

SPECIFIC APPLICATIONS

Outcropping

Layered models of stratified flow have been favored by theoreticians because of their conceptual simplicity, but have only seen limited use until recently in numerical modeling due to difficulties related to layer outcropping (vanishing layer depth). Two mass transport schemes capable of handling outcropping, the Flux Corrected Transport (FCT) and the MPDATA algorithms, were tested against analytic solutions describing wind- and buoyancy-forced flows.[10]

The essential aspects of the circulation[29,30,31] in a two-layer, two-gyre wind-forced ocean basin (one aspect being the size of the outcrop region) are controlled by a single nondimensional number $\lambda = \tau_m L/g' H_1^2$ where τ_m is the maximum wind stress; L the basin width; $g' = g\Delta\rho/\rho$ the buoyancy difference between the two layers, and H_1 the mean upper-layer thickness. In order to illustrate the model's ability to handle zero layer thicknesses, one of the analytic solutions[29] for a finite-depth lower layer (Figure 1 a,b) has been reproduced numerically. The parameters τ_m, L and g' were chosen such that $\lambda = 0.30$ yields an outcrop region which spans virtually the entire cyclonically-forced northern half of the domain region and extends into the anticyclonically-forced southern half (Figure 1 a,b). After approximately 5 years of integration starting from rest, the model reached a steady state characterized by upper- and lower-layer mass transport streamfunctions shown in Figure 1 c,d. These model results were obtained with the Flux Corrected Transport algorithm. As in the analytic solution (Figure 1 a,b), the outcrop area in both figures is observed to extend south of the latitude of maximum wind stress (the zero wind stress curl line, ZWCL). The upper- and lower-layer flow combine to reduce the total mass flux across the ZWCL to zero, satisfying the Sverdrup balance. This result combined with others[10] alleviates longstanding reservations about the severity of the outcrop problem in layer models.

Bottom Topography

Another aspect which also retarded the development of layered models is the difficulty associated with isopycnal intersecting steep topography. Not only does one need to accomodate regions of zero isopycnal layer thickness in the presence of topography, but also the drag exerted laterally by steep slopes must be taken into account whenever bottom topography affects layer thickness.[29] The model's ability to handle this aspect was well illustrated in a series of experiments performed in a 4000 meter deep periodic channel with a tall isolated seamount at the center and with 15 constant-density layers in the vertical.[32] The Coriolis parameter, fluid stratification, coefficient of lateral friction and length scale of the topography were held constant, while the mean downstream flow speed and height of the obstacle varied up to an extreme case of a 20 cm s^{-1} current impinging on a 3500 m seamount.

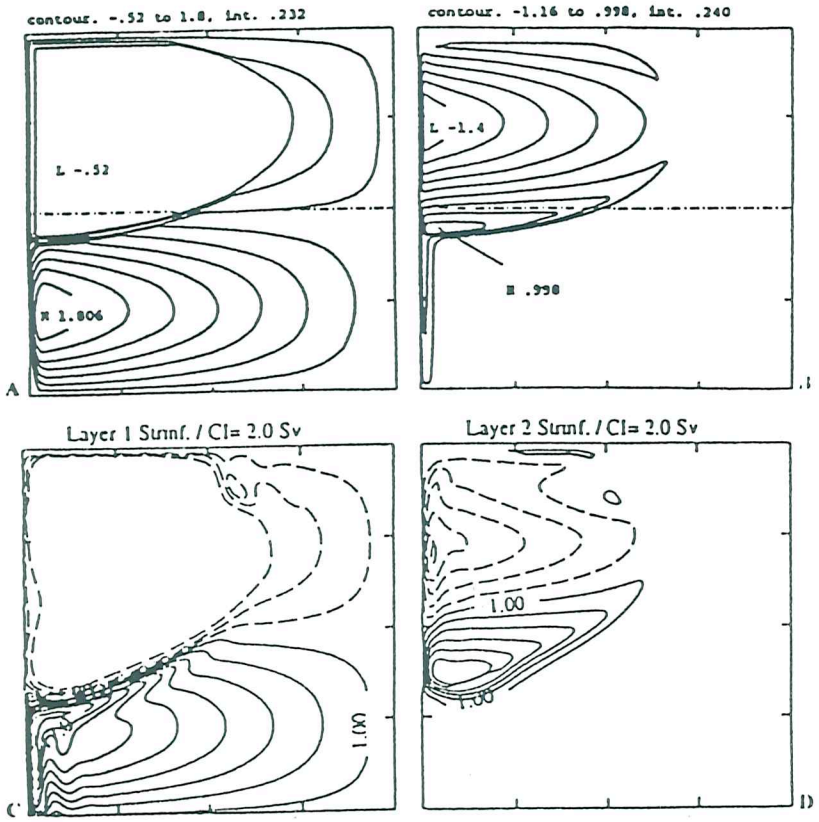

FIGURE 1. Mass transport stream function in upper layer (left) and lower layer (right). (a,b) analytic solution (nondimensional units correspond approximately to 12 × $10^6 m^3 s^{-1}$); (c,d) numerical solution using the Flux Corrected Transport algorithm.

The cross-stream vertical section through flow near the tall seamount in Figure 2 illustrates the model's behavior in the presence of isopycnals intersecting steep topography. The behavior of the fluid is found to differ little from simulations with smaller seamounts, as far as the formation and interaction of relative vorticity anomalies over and in the lee of the obstacle and the downstream transport of a cyclonic vortex are concerned.[32,33]

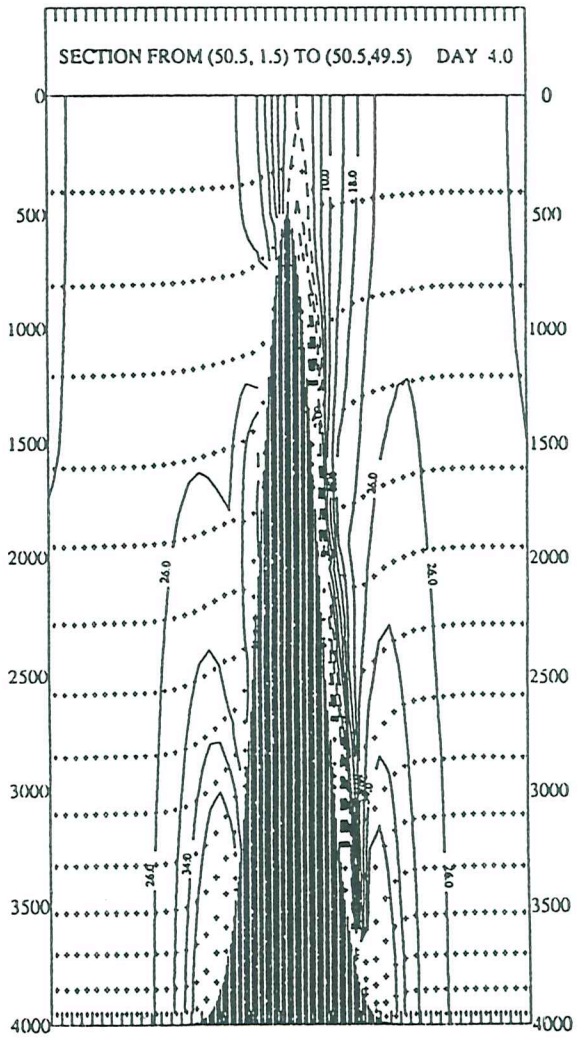

FIGURE 2. Cross-stream vertical section through center of seamount. Plus signs denote layer interfaces. Solid isotachs denote flow away from viewer; contour interval 4 $cm\ s^{-1}$.

A SIMULATION OF THE ATLANTIC OCEAN

As part of a multi-year, multi-institutional series of model applications and analyses, with the goal of establishing a sequence of eddy-resolving baseline calculations of the wind- and thermohaline-driven large scale ocean circulation, both the University of Miami and the Rennell Centre for Ocean Circulation in Southampton, England, are presently performing high resolution simulations of the circulation in the Northern and Equatorial Atlantic on decadal time scales using the above isopycnic-coordinate model. A similar experiment was completed a few years ago at the National Center for Atmospheric Research (NCAR) with the z-coordinate primitive-equation model developed at the Geophysical Fluid Dynamics Laboratory (GFDL).[14] Until recently, the GFDL model was the only "general-purpose" numerical model available to the physical oceanography community. The main purpose of the Miami and Southampton simulations is to answer questions concerning the degree to which the numerical representation of physical processes affects the realism of the numerical solution.

The simulation described in the remainder of this section covers the Atlantic between approximately 80°N (the Fram strait) and 15°S. The domain is spanned by a 1° mesh consisting of 126 by 103 grid points.[39] No artificial smoothing has been applied to the bathymetry, so that the features are relatively steep and complex. The model comprises a total of 20 layers: a Kraus-Turner-type mixed layer (vertically homogeneous but of density varying in the horizontal) and 19 isopycnic layers with potential density values of 25.65-27.75$kg\ m^{-3}$ in increments of 0.15, and from 27.75-28.15$kg\ m^{-3}$ in increments of 0.10 (the densities are specified with the two leading digits omitted following standard oceanographic practice). The model, started from a state of rest and spun up for a period of 30 years, was initialized from the September temperature, salinity and interface depth values of the Levitus dataset.[13] The base of the mixed layer was initially defined to coincide with the 25.575 density surface, or 50m, whichever was deeper.

The forcing functions driving the circulation are based on interpolations onto the model grid of the Hellerman and Rosenstein winds,[16] the Esbensen and Kushnir heat fluxes,[17] and the Jaeger precipitation[18] minus the Esbensen and Kushnir evaporation fields. Thermodynamic fluxes applied at the sea surface are based on the above plus a correction term which provides a moderate and partial relaxation (with approximately a 4-month timescale for a 100m thick water column) of the mixed layer temperature and salinity to Levitus climatology. The ocean interior, on the other hand, is not relaxed to climatological conditions in any way.

The northern and southern boundaries are represented by solid walls and no thermodynamic restoration was employed, so that no lateral fluxes of either heat or salt were allowed in or out of the model domain. At all lateral boundaries of the model domain, including coastlines and islands, a no slip condition was used for the velocity fields. Finally, a simple sea-ice model was incorporated into the code for the present integration.

Figure 3 shows the mixed layer velocity patterns in March after 30 years of integration. A prominent feature is of course the Gulf Stream, which flows up the

coast of Florida and separates from the US shelf at about 40°N, near Cape Cod. This is somewhat too far north (satellite imagery indicating separation at Cape Hatteras, about 34°N) but is in line with results from other models.[34,40,41] The transport in the Gulf Stream is about 33 Sv at 26°N, increases steadily to about 45 Sv at 32°N, also in general agreement with the results of other studies. After separation from the coast, the current is associated with a marked temperature front extending across much of the central Atlantic and separating the cyclonic subpolar gyre to the north from the anticyclonic subtropical gyre to the south. Other features worth noting are the equatorial current system producing a strong North Brazil current, and upwelling resulting from divergence of the surface currents, at both the equator and off the coast of Africa, both being known phenomena.

The model mixed layer depth fields after 30 years of integration are compared with observations in Figure 4. The observations[42] show the deepest mixing in an area occupied by water with densities in excess of 27.75. This region covers most of the Labrador basin, but also extends in a thin tongue around Cape Farewell into the Irminger basin. This near correspondence between mixing in excess of 1000m and densities above 27.75 is also seen in the model results, even though the area over which this occurs in the model is somewhat smaller in the Labrador basin and more pronounced in the Irminger basin. Overall, the agreement between the observations and the model output in the mixed layer is quite good.

The model's representation of the annual cycle of mixed layer deepening and retreat is shown schematically in Figure 5. Layer interfaces are shown in these sections, which cut through the top 2400m of the model domain, as solid

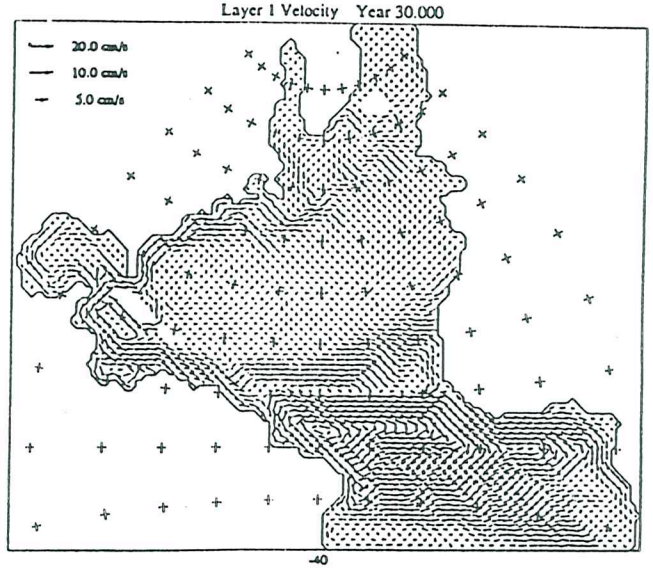

FIGURE 3. Mixed-layer velocities in March of year 30 (Rennell Centre simulation).

lines; isotherms are dashed. The stairsteps built into the isotherms are intentional: they illustrate the fact that T is a layer variable in the model and thus piecewise constant in the vertical. Stairsteps have been rounded off to improve legibility.

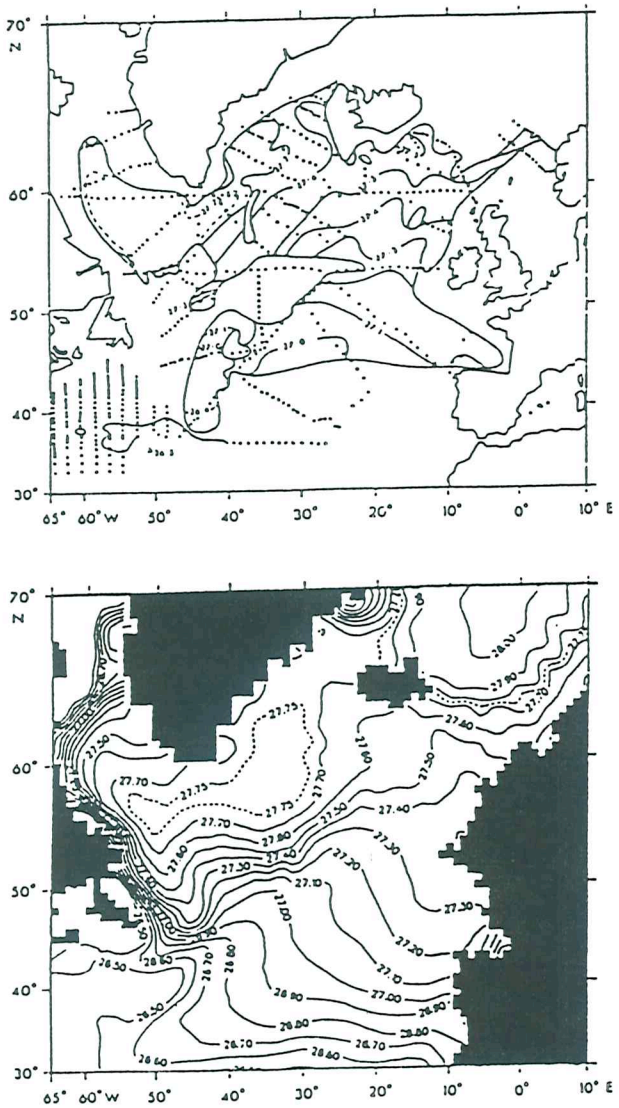

FIGURE 4. Wintertime mixed-layer density: (a) observed; (b) from numerical simulation in March of year 30. Contour interval: 0.1$kg\ m^{-3}$, additional 27.75 contour added (dashed).

In late winter (Figure 5a), the interface marking the mixed layer bottom is sharply inclined polewards of 50°N, allowing the mixed layer to reach depths in excess of 1000m. In summer (Figure 5b), almost the entire volume occupied by the subpolar wintertime mixed layer is seen to be filled with isopycnal layers; a seasonal thermocline has formed. Layer interfaces there rise sharply to the surface in a manner reminiscent of the wintertime mixed-layer isotherms.

The "bowl" formed by the upper isopycnic layers between 15°N and 50°N in Figure 5b represents the (primarily wind-driven) subtropical gyre. Figure 5a shows that this bowl is truncated along its northern edge by the wintertime mixed layer;

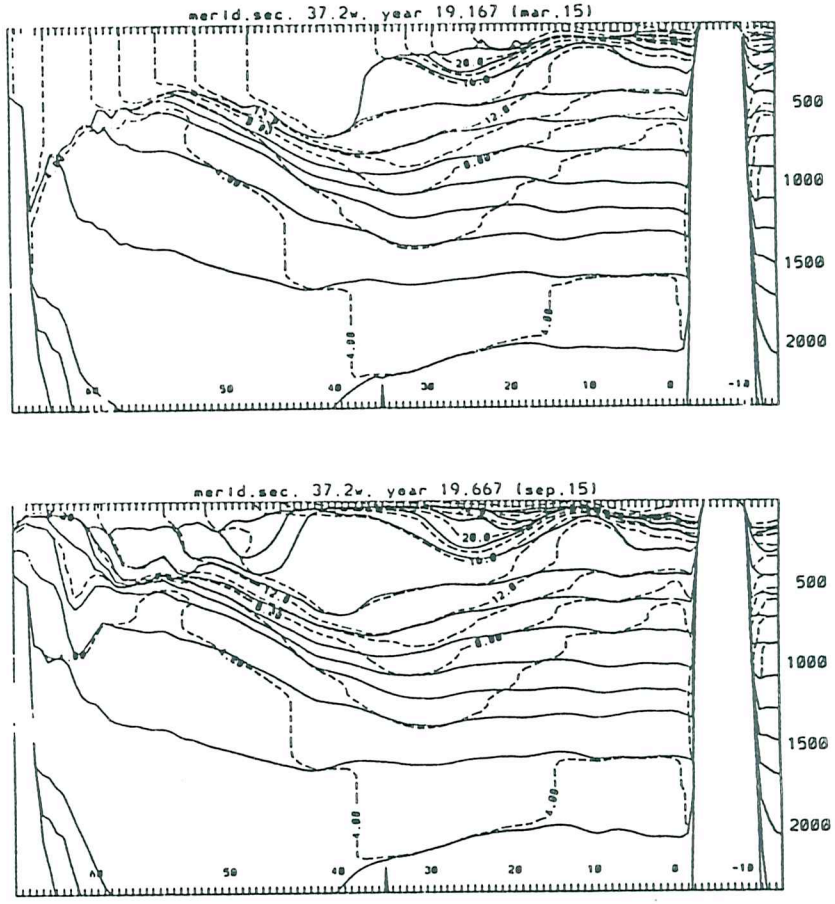

FIGURE 5. Vertical-meridional section through model grid along 34.5°W (a) in March and (b) in September of year 19. Solid lines: layer interfaces; dashed lines: isotherms. The sharp rise south of the equator corresponds to the eastern tip of the South American continent.

that this bowl is truncated along its northern edge by the wintertime mixed layer; in other words, the bowl resides partly in the seasonal and partly in the permanent thermocline. The fact that the surface mixed layer reaches down into the subtropical gyre on an annual basis means that the subtropical gyre is a "ventilated" body of water.

OUTLOOK

Recognition of the quasi-adiabatic character of oceanic motion on fairly long time scales has encouraged the use of layer models in studying dynamic interaction modes, but a variety of technical difficulties has impeded their development into full-fledged OGCMs. Most of these difficulties have been overcome by now. The intrinsic capacity of layer models to dynamically adapt their spatial vertical resolution to the occurrence of baroclinic zones, as well as the prospect of being able to handle long-term climate-oriented OGCM integrations in a framework where diabatic exchange processes are totally under the experimenter's control, has encouraged several modeling groups to pursue the development of practical isopycnic OGCM codes to study the oceanic circulation on time scales ranging from days to centuries.

At the time of this writing, both the Miami and the Rennell group are gearing up for basin-scale, eddy-resolving simulations. The Miami group intends to do its simulations on a massively parellel processor (MPP). During the past year, the Los Alamos National Laboratory has provided generous programmer assistance to port the Miami model to one particular MPP, the CM-5 built by Thinking Machines Inc. Array sizes on a Connection Machine must be padded to the next power of 2 for good performance, implying that an ocean basin fitting snugly into an array of size $2^m \times 2^n$ minimizes the number of unused processors. (Many processors remain unused as it is because they end up on dry land.)

A 0.9-degree version of the model (128 x 128 horizontal grid points) runs on 64 nodes of the CM-5 at 1.3 times the speed of a single-processor Cray Y-MP, or 3.5 hrs. per model year. Optimal machine utilization will be reached with a further doubling of the horizontal grid resolution. To achieve satisfactory eddy resolution, the number of horizontal grid points will have to be quadrupled (0.225-degree mesh).

ACKNOWLEDGEMENTS

Many co-workers contributed toward the development of the Miami model in the past ten years as well as to the results presented in this chapter. To name a few, we would like to acknowledge the late D. Boudra, A. Bennett, S. Dean, H. Hanson, D. Hu, E. Kraus, K. Maillet, A. New, C. Rooth, L. Smith and S. Sun. Support was provided by the National Science Foundation, the Office of Naval Research and the Department of Energy.

REFERENCES

1. Bryan K. 1969. A numerical method for the study of the circulation of the world ocean. *J. Comput. Phys.*, 4,347-376.
2. Phillips, N.A. 1957. A coordinate system having some special advantages for numerical forecasting. *J. Meteor.*, 14,184-185.
3. Blumberg, A.F. and G.L. Mellor. 1987. A description of a three-dimensional coastal ocean circulation model. *Three-Dimensional Coastal Ocean Models*, 4, edited by N. Heaps. American Geophysical Union, 208 pp.
4. Haidvogel, D.B., J. Wilkin and R. Young. 1991. A semi-spectral primitive equation ocean circulation model using vertical sigma and orthogonal curvilinear horizontal coordinates. *J. Comp. Phys.*, 94,151-185.
5. Montgomery, R.B. 1937. A suggested method for representing gradient flow in isentropic surfaces. *Bull. Amer. Meteor. Soc.*, 18,210-212.
6. Bleck, R. and D.B. Boudra. 1981. Initial testing of a numerical ocean circulation model using a hybrid (quasi-isopycnic) vertical coordinate. *J. Phys. Oeanogr.*, 11,755-770.
7. Bleck, R. and D.B. Boudra. 1986. Wind-driven spin-up in eddy-resolving ocean models formulated in isopycnic and isobaric coordinates. *J. Geophys. Res.*, 91C,7611-7621.
8. Zalesak, S. 1979. Fully multidimensional flux-corrected transport algorithms for fluids. *J. Comp. Phys.*, 31,335-362.
9. Smolarkiewicz, P. 1984. A fully multidimensional positive definite advection transport algorithm with small implicit diffusion. *J. Comput. Phys.*, 54,325-362.
10. Sun, S., R. Bleck and E.P. Chassignet. 1993. Layer outcropping in numerical models of stratified flows. *J. Phys. Oceanogr.*, 23, 1877-1884.
11. Luyten, J.R., J. Pedlosky and H. Stommel. 1983. The ventilated thermocline. *J. Phys. Oceanogr.*, 13,292-309.
12. Luther, M.E. and J.J. O'Brien. 1985. A model of the seasonal circulation in the Arabian Sea forced by observed winds. *Prog. Oceanogr.*, 14,353-385.
13. Jensen, T.G. 1991. Modeling the seasonal undercurrents in the Somali Current system. *J. Geophys. Res.*, 96,22151-22167.
14. Hurlburt, H.E. and J.D. Thompson, 1980. A numerical study of loop intrusions and eddy shedding. *J. Phys. Oceanogr.*, 10,1611-1651.
15. Thompson, J.D. and W.J. Schmitz. 1989. A limited-area model of the Gulf Stream: Design, initial experiments, and model-data intercomparison. *J. Phys. Oceanogr.*, 19,791-814.
16. McCreary, J.P. and P.K. Kundu. 1988. A numerical investigation of the Somali current during the Southwest Monoon. *J. Mar. Res*, 46,25-58.
17. Bennett, A. 1992. Personal communication.
18. Oberhuber, J. 1993. Simulation of the Atlantic circulation with a coupled sea ice - mixed layer - isopycnal general circulation model. Part I and II. *J. Phys. Oceanogr.*, 23,808-845.
19. Bleck, R. H.P. Hanson, D. Hu and E.B. Kraus. 1989. Mixed layer-thermocline interaction in a three-dimensional isopycnic coordinate model, *J. Phys.*

Oceanogr., 19,1417-1439.
20. Bleck, R. and L. Smith. 1990. A wind-driven isopycnic coordinate model of the north and equatorial Atlantic Ocean. 1. Model development and supporting experiments. *J. Geophys. Res.*, 95C, 3273-3285.
21. Bleck, R., C. Rooth, D. Hu and L. Smith. 1992. Salinity-driven thermocline transients in a wind- and thermohaline-forced isopycnic coordinate model of the North Atlantic. *J. Phys. Oceanogr.*, 22,1486-1505.
22. Bleck, R. 1978. Finite difference equations in generalized vertical coordinates. Part I: Total energy conservation. *Contrib. Atm. Phys.*, 51, 360-372.
23. Arakawa, A. and V.R. Lamb. 1977. Computational design of the basic processes of the UCLA general circulation model, *Methods Comput. Phys.*, 17,174-265.
24. Kraus, E.B. and J.S. Turner. 1967. A one-dimensional model of the seasonal thermocline: II. The general theory and its consequences. *Tellus*, 19,98-106.
25. Friedrich, H. and S. Levitus. 1972. An approximation to the equation of state for sea water, suitable for numercial ocean models. *J. Phys. Oceanogr.*, 2,514-517.
26. Smolarkiewicz, P. and W. Grabowski. 1990. The multidimensional positive definite advection transport algorithm: Nonoscillatory option. *J. Comput. Phys.*, 86,355-375.
27. Smagorinsky, J.S. 1963. General circulation experiments with the primitive equations. I: The basic experiment. *Mon. Wea. Rev.*, 91,99-164.
28. Hu, D. 1991. A joint mixed-layer/isopycnic coordinate numerical model of wind- and thermohaline-driven ocean general circulation with model sensitivity study. Ph. D. dissertation. U. of Miami. 220 pp.
29. Huang, R.X. 1984. The thermocline and current structure in subtropical/subpolar basins. Ph.D. thesis, WHOI-84-42, 218 pp.
30. Huang, R.X. 1986. Numerical simulation of wind-driven circulation in a subtropical/subpolar basin, *J. Phys. Oceanogr.*, 16,1636-1650.
31. Huang, R.X. and G. Flierl. 1987. Two-layer models for the thermocline and current structure in subtropical/subpolar gyres. *J. Phys. Oceanogr.*, 17,872-884.
32. Smith, L.T. 1992. Numerical simulations of stratified rotating over finite amplitude topography. *J. Phys. Oceanogr.*,22,686-696.
33. Huppert, H.E. and K. Bryan. 1976. Topographically generated eddies. *Deep-Sea Res.*, 23,655-679.
34. Bryan, F.O. and W.R. Holland. 1989. A high resolution simulation of the wind- and thermohaline-driven circulation in the North Atlantic Ocean. In *Parameterization of Small Scale Processes.* Proceedings Aha Huliko'a Hawaiian Winter Workshop. U. of Hawaii. January 17-20, 1989. P. Muller and D. Anderson, Eds.
35. Levitus, S. 1982. *Climatological Atlas of the World Ocean.* NOAA Professional Paper 13, 173 pp.
36. Hellerman, S. and M. Rosenstein. 1983. Normal monthly wind stress over the World Ocean with error estimates. *J. Phys. Oceanogr.*, 13,1093-1104.
37. Esbensen, S.K. and Y. Kushnir. 1981. Heat budget of the global ocean: estimates from surface marine observations. Rep. No. 29, Climatic Research Institute, Oregon State University, Corvallis, OR, 27 pp.

38. Jaeger, L. 1976. Monatskarten des Niederschlags fur die ganze Erde. Berichte des Deutschen Wetterdienstes, 18, No. 139, Ofenbach, FRG.
39. New, A., R. Bleck, Y. Jia, R. Marsh, M. Huddleston and S. Barnard. 1994. An isopycnic model study of the North Atlantic. Part 1: Model experiment and water mass formation. Part 2: Interdecadal variability of the subtropical gyre. *J. Phys. Oceanogr.*, submitted.
40. Semtner, A.J. and R.M. Chervin. 1988. A simulation of the global ocean circulation with resolved eddies. *J. Geophys. Res.*, 93,15502-15522.
41. Semtner, A.J. and R.M. Chervin. 1992. Ocean general circulation from a global eddy-resolving model. *J. Geophys. Res.*, 97,5493-5550.
42. McCartney, M.S. and L.D. Talley, 1982. The subpolar mode water of the North Atlantic Ocean. *J. Phys. Oceanogr.*, 12,1169-1188.